E3 ligase recruitment by UBQLN2 protects substrates from proteasomal degradation

Ashley Scheutzow[1,2]*, Sachini Thanthirige[1,3]*, Gracie Siffer[1,4], and Matthew L. Wohlever[1,3]

[1]Previously at University of Toledo, Department of Chemistry & Biochemistry
[2]University of Michigan Medical School, Department of Biological Chemistry
[2]University of Pittsburgh, Department of Cell Biology
[4]Northwestern University, Department of Molecular Biosciences
*These authors contributed equally

Abstract
Ubiquilins are a family of proteins critical to cellular proteostasis that are also linked to neurodegenerative diseases such as ALS, with specific mutations in UBQLN2 causing dominant, X-linked ALS. Despite an initial characterization as proteasomal shuttle factors, Ubiquilins have paradoxically been reported to stabilize numerous substrates. The basis of this triage decision remains enigmatic. Many other fundamental aspects of Ubiquilin function are unclear at the mechanistic level, such as the physiological significance of Ubiquilin phase separation, the unique role of each Ubiquilin paralog, and the mechanistic defects of ALS mutants. To address these questions, we utilized a library of triple knockout (TKO) rescue cell lines with physiological expression of single Ubiquilin paralogs or disease mutants in an isogenic background. Our findings reveal that UBQLN2 has a unique ability to protect substrates from degradation and that substrate stabilization correlates with the recruitment of multiple E3 ligases, including SCF^{bxo7}. Substrate stabilization is diminished in ALS mutants and this defect is exacerbated upon overexpression. We propose that UBQLN2 is a molecular chaperone that recruits multiple E3 ligases to modulate substrate stability. This proposal unifies many existing observations in the field and presents a new paradigm for understanding Ubiquilin function in health and disease.

Introduction

Protein homeostasis (proteostasis) involves a complex network of cellular pathways responsible for the synthesis, folding, and degradation of proteins[1–5]. Failures in this essential process lead to numerous neurodegenerative diseases, including Amyotrophic Lateral Sclerosis (ALS)[6–12]. Ubiquilins are a family of proteins at the nexus of the cellular proteostasis network, with connections to the ubiquitin proteasome system, autophagy, and the pathological protein aggregates characteristic of various proteinopathies[13–18]. Humans have three widely expressed Ubiquilin paralogs, UBQLN1, UBQLN2, and UBQLN4. The unique role of each paralog is poorly understood, although UBQLN2 has garnered significant attention as point mutations lead to dominant, X-linked ALS[19–25]. These mutations lead to the formation of protein aggregates that are a hallmark of ALS pathology, but the precise mechanisms by which UBQLN2 mutations contribute to ALS remain enigmatic[26–29].

Ubiquilins were originally characterized as proteasomal shuttle factors that facilitate protein degradation, with the Ubiquitin Like (UBL) domain binding the proteasome and the Ubiquitin Associated (UBA) domain binding to ubiquitinated proteins[30,31]. The middle region of the protein contains two Sti1 domains which are important for binding to hydrophobic transmembrane domains (TMDs)[32]. Several groups have previously shown that the UBA domain can also recruit E3 ligases, although the functional role of E3 ligase recruitment is unknown[32,33]. Despite the initial characterization as shuttle factors and the association with E3 ligases, Ubiquilins have paradoxically been shown to stabilize numerous substrates[29,34–39]. Why some substrates are stabilized and others are degraded is unknown.

Another defining feature of Ubiquilins is the ability to undergo phase separation and form biomolecular condensates[13]. The role of phase separation in Ubiquilin activity is unclear, although there are hints that it is linked to the substrate triage decision. For example, Ubiquilin phase separation is modulated by polyubiquitin chains in a linkage dependent manner and proteasome activity can be inhibited in Ubiquilin condensates[40,41]. Interestingly, many ALS mutants show altered phase separation properties[23,26,42]. As Ubiquilin phase separation is concentration dependent, care must be taken to replicate physiological Ubiquilin expression levels.

Here, we use a library of triple knockout (TKO) rescue cell lines that have physiological expression of a single Ubiquilin paralog or disease mutant in an isogenic background[32]. Using this library, we show that TKO cells rescued with UBQLN2 have a unique ability to protect substrates from proteasomal degradation and that substrate stabilization correlates with both UBQLN2 expression levels and E3 ligase recruitment. We show that Ubiquilins recruit multiple E3 ligases, including SCF^{bxo7}, which is recruited in its activated form. Finally, we show that UBQLN2 ALS mutants have a reduced ability to stabilize substrates.

Results

Cells expressing only UBQLN2 show growth defects

To examine the unique functional role of the different Ubiquilin paralogs, we used the TRex Flp-In system to generate triple knockout rescue HEK cell lines **(Figure 1A)**. The triple knockout (TKO) cells have UBQLN1, 2, and 4 deleted and are then complemented with a single Myc-tagged Ubiquilin variant that is chromosomally integrated and under control of a doxycycline inducible promoter[32]. We will refer to the rescue cell lines as TKO^{UBQLN-}, with the superscript describing the Ubiquilin variant used for complementation. Importantly, all integrations occur at the same chromosomal locus, so all cell lines are isogenic except for the Ubiquilin of interest.

As Ubiquilins are known to undergo phase separation in a concentration dependent manner, we first sought to define the concentration of doxycycline required for physiological expression. Using anti-UBQLN2, and anti-UBQLN4 antibodies, we determined that 10 ng/mL doxycycline gave physiological expression levels of UBQLN1 and UBQLN4 whereas 0.8 ng/mL doxycycline was required to give physiological expression of UBQLN2 **(Figures 1B-D)**. As many previous studies used transient overexpression of UBQLN2, we decided to study rescue cells expressing UBQLN2 at physiological levels (0.8 ng/mL) and overexpression conditions (10 ng/mL), which we will refer to as TKO^{UBQLN2} and $TKO^{UBQLN2\text{-}High}$ respectively.

With our expression conditions firmly established, we first examined the fitness of the TKO rescue cells. Consistent with previous reports, TKO cells showed a significant growth defect whereas TKO^{UBQLN1} and TKO^{UBQLN4} cells showed little to no fitness defect under standard growth conditions. Surprisingly, TKO^{UBQLN2} cells showed an intermediate phenotype between WT HEK cells and TKO cells **(Figure 1E)**. This effect was not dependent on UBQLN2 overexpression as $TKO^{UBQLN2\text{-}High}$ had the same growth rate.

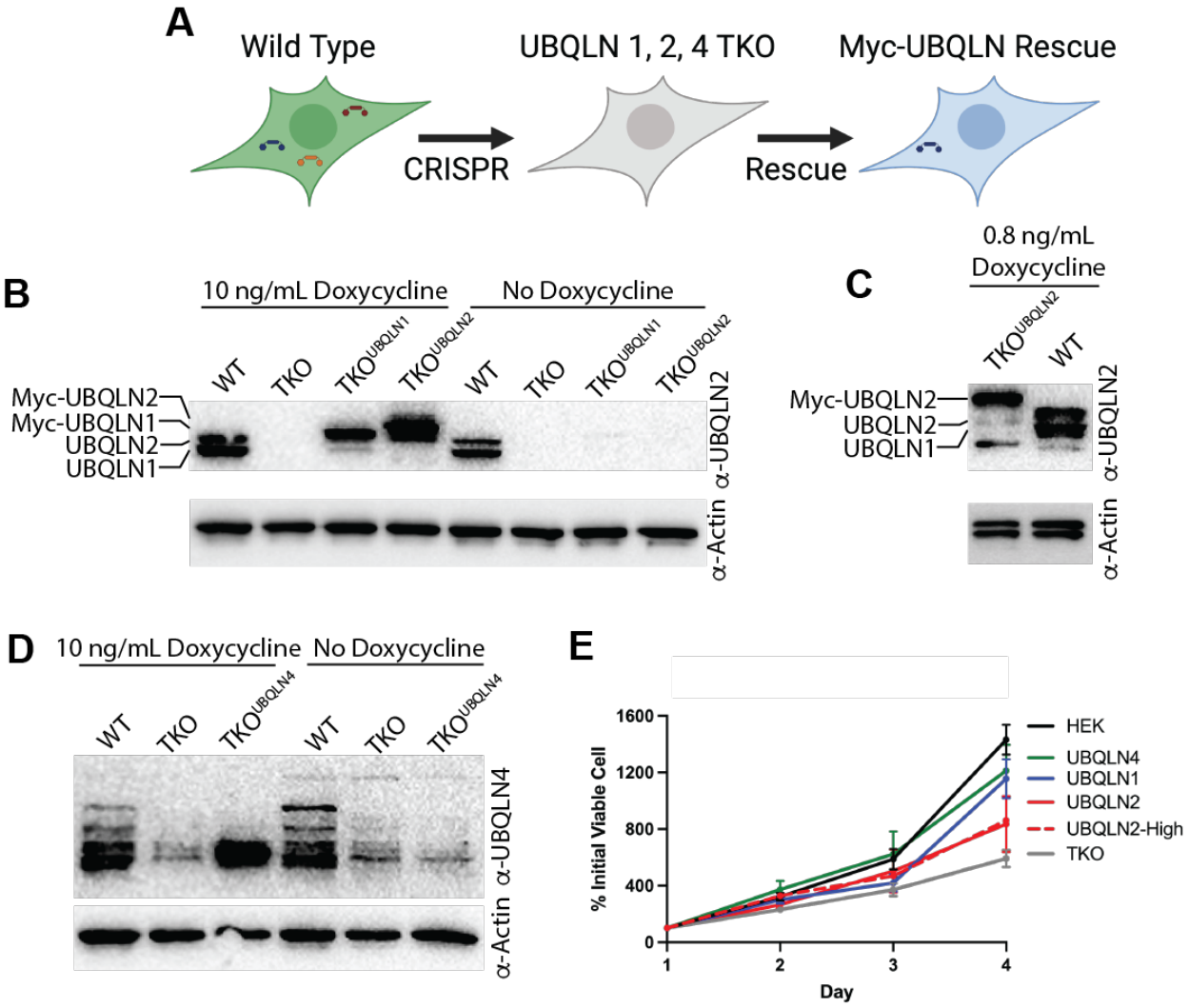

Figure 1: Development of TKO rescue cell lines with physiological and overexpression of individual ubiquilins

a) Diagram of TKO rescue strategy.

b) TKO^{UBQLN1} cells require 10 ng/mL of doxycycline to have physiological Ubiquilin expression levels. TKO^{UBQLN2} cells show overexpression under these conditions. Anti-UBQLN2 western blot of cells treated with 10 ng/mL doxycycline
c) TKO^{UBQLN2} cells require 0.8 ng/mL of doxycycline to have physiological Ubiquilin expression level. Anti-UBQLN2 western blot of cells treated with 0.8 ng/mL doxycycline
d) TKO^{UBQLN4} cells require 10 ng/mL of doxycycline to have physiological Ubiquilin expression levels. Anti-UBQLN4 western blot with 10 ng/mL doxycycline
e) Growth curves of WT, TKO, TKO^{UBQLN1}, TKO^{UBQLN2}, TKO^{UBQLN4}, $TKO^{UBQLN2\text{-}High}$ cells. Cell viability was measured with a hemocytometer and trypan blue staining.

<u>UBQLN2 protects client proteins from proteasomal degradation</u>

We next asked if the growth defect in the TKO^{UBQLN2} cell line was due to changes in proteostasis capacity. As a model substrate, we used mitochondrial membrane protein ATP5G1 with the mitochondrial targeting sequence deleted (ATP5G1ΔMTS), as this protein was previously shown to bind to Ubiquilins[32]. To assess the ability of Ubiquilins to facilitate degradation of ATP5G1ΔMTS we used a ratiometric fluorescent reporter containing an in frame-fusion of GFP-ATP5G1ΔMTS and mCherry separated by the viral 2A sequence[43] **(Figure 2A)**. GFP-ATP5G1ΔMTS and mCherry are expressed at equal levels, but as separate protein products, thus providing an internal expression control. The GFP:mCherry ratio in each cell can be quantitatively measured by flow cytometry. Control experiments with untagged GFP showed nearly identical GFP/mCherry ratios between all cell lines, regardless of Ubiquilin expression **(Figure S1)**.

We transfected the GFP-ATP5G1ΔMTS-P2A-mCherry construct in WT, TKO, and TKO rescue cell lines. The GFP:mCherry ratio decreased from ~1 to ~0.5 in the TKO cells, suggesting Ubiquilin independent degradation **(Figure 2B)**. We observed modest, but reproducible decreases in the GFP/mCherry ratio in WT and TKO^{UBQLN1} cells compared to TKO cells, suggesting that UBQLN1 facilitates ATP5G1ΔMTS degradation, consistent with previous studies[32]. GFP/mCherry ratios in TKO^{UBQLN4} cells were slightly elevated compared to the TKO cells.

Strikingly, we observed that ATP5G1ΔMTS was dramatically stabilized in the TKO^{UBQLN2} with the degree of substrate stabilization correlating with UBQLN2 expression levels **(Figure 2B)**. Because the overall increase in GFP:mCherry ratio far exceeded the level in TKO cells, we conclude that UBQLN2 is actively protecting substrates from degradation rather than acting via a simple loss of function.

We next asked how UBQLN2 can protect substrates from degradation. As Ubiquilins can bind to the proteasome, we hypothesized that UBQLN2 could be protecting client proteins from proteasomal degradation. Indeed, Valentino et al. recently reported that UBQLN2 can recruit the 26S proteasome into biomolecular condensates, which can inhibit proteasome activity of K63 linked or mixed-linkage substrates[40]. Such a model makes several predictions, including: 1) there should be a unique accumulation of ubiquitinated substrates in TKO^{UBQLN2} cells, 2) proteasome inhibitors should produce no further substrate stabilization, and 3) K63 ubiquitin linkages will enhance substrate stabilization.

To query the ubiquitination state of the substrates, we performed a cell-based ubiquitination assay. TKO rescue cell lines were co-transfected with the GFP-ATP5G1ΔMTS-P2A-mCherry and HA-Ubiquitin. GFP-ATP5G1ΔMTS was immunoprecipitated in the absence of any proteasome inhibitors. We observed a hyperaccumulation of ubiquitinated substrate only in

TKO^{UBQLN2} cells, with the degree of accumulation correlating with the level of UBQLN2 expression **(Figure 2C)**.

We then repeated the cell-based ubiquitination assay in cells treated with the proteasome inhibitor MG132 **(Figure 2D)**. Proteasome inhibition increased the accumulation of ubiquitinated substrates in HEK, TKO, and TKO^{UBQLN1} cell lines, suggesting that ATP5G1ΔMTS is subject to proteasomal degradation in these cell lines. Conversely, addition of MG132 led to a modest decrease in the amount of ubiquitinated ATP5G1ΔMTS in TKO^{UBQLN2} cells.

To test if K63 ubiquitin linkages enhance substrate stabilization, we repeated the cell-based ubiquitination assay with TKO^{UBQLN2} cells transfected with WT or K63-only HA-Ubiquitin. Consistent with our model, we saw an increase in ubiquitinated substrates when cells were transfected with K63-only ubiquitin compared to wild type ubiquitin **(Figure 2E)**. We conclude that rather than acting as a proteasomal shuttle factor, UBQLN2 actively protects ubiquitinated substrates from proteasomal degradation.

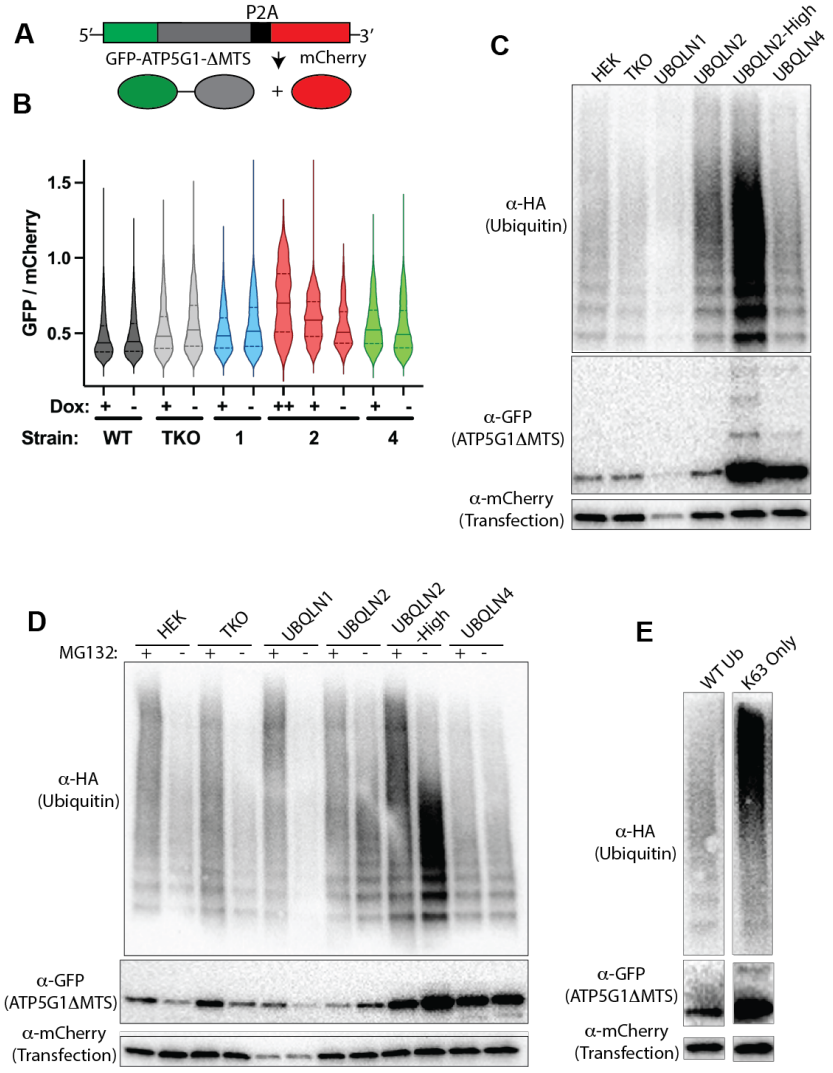

Figure 2: TKO^{UBQLN2} cells have an accumulation of ubiquitinated substrates

a) Diagram of the GFP-mCherry assay

b) TKO^{UBQLN2} cells (red) show a dramatic stabilization of the substrate that correlates with UBQLN2 expression levels. Doxycycline concentrations were sufficient to give physiological Ubiquilin expression (+) or overexpression (++). Note that the GFP/mCherry ratio is much higher than in the TKO cells, suggesting that this is not a simple loss of function.
c) TKO^{UBQLN2} cells have an accumulation of ubiquitinated substrates that correlates with UBQLN2 expression levels. The GFP-ATP5G1ΔMTS-P2A-mCherry substrate was co-transfected with HA-Ubiquitin. GFP immunoprecipitation shows an accumulation of Ubiquitinated substrates in TKO^{UBQLN2} cells.
d) Proteasome inhibition does not increase the amount of ubiquitinated substrate in TKO^{UBQLN2} cells. Assay performed as in C, except cells were treated with MG132 or DMSO for 4 hours prior to harvesting.
e) K63 promotes the accumulation of ubiquitinated substrates. Cell-based ubiquitination assay performed in TKO^{UBQLN2} cells co-transfected with GFP-ATP5G1ΔMTS-P2A-mCherry substrate and either WT or K63-only HA-Ubiquitin. Images were cropped from the same western with the same contrast adjustment.

Substrate stabilization correlates with E3 ligase recruitment

We next asked what is unique about UBQLN2 that allows it to protect substrates from proteasomal degradation. Previous reports had demonstrated that UBQLN2 condensates can inhibit the 26S proteasome and UBQLN2 phase separation is enhanced by polyubiquitin chains[40,44–46]. Furthermore, we and others had previously demonstrated that Ubiquilins use the UBA domain to recruit an E3 ligase[32,33]. We therefore hypothesized that the accumulation of ubiquitinated substrates in TKO^{UBQLN2} cells was due to enhanced E3 ligase recruitment by UBQLN2. This model predicts that substrate stabilization depends on E3 ligase recruitment by UBQLN2 and that UBQLN2 can recruit E3 ligases more robustly than other Ubiquilin paralogs.

To test if E3 ligase recruitment is essential for the accumulation of ubiquitinated substrates, we performed our cell-based ubiquitination assay with $TKO^{UBQLN2\Delta UBA}$ cells. As the UBA domain is essential for E3 ligase recruitment, there should be a reduction in the amount of ubiquitinated substrate in these cells. Consistent with our model, we observed a substantial drop in ubiquitinated substrates compared to the TKO^{UBQLN2} control **(Figure 3A)**.

To test if UBQLN2 can recruit E3 ligases more robustly than other Ubiquilin paralogs, we performed an *in vitro* ubiquitination assay **(Figure 3B)**. In this assay, the known Ubiquilin substrate Omp25 is generated by in vitro translation (IVT) in rabbit reticulocyte lysate (RRL) supplemented with physiological concentrations of flag-tagged Ubiquilin. Previous results had demonstrated that the UBL domain is a negative regulator of E3 ligase recruitment, so the ΔUBL construct was used as a positive control and ΔUBA as a negative control[32]. Ubiquilin substrate complexes were purified by anti-flag immunoprecipitation and the eluate was complimented with purified E1 (Ube1), E2 (UbcH5A), Ubiquitin, and ATP. Ubiquitination activity was analyzed by anti-ubiquitin western blot. As no E3 ligase was added, any ubiquitination activity must result from an E3 ligase that co-immunoprecipitated with Ubiquilin. Consistent with our hypothesis, UBQLN2 constructs had the highest level of ubiquitination activity **(Figure 3C)**. We conclude that UBQLN2 has a unique ability to recruit E3 ligases, which correlates with substrate stabilization.

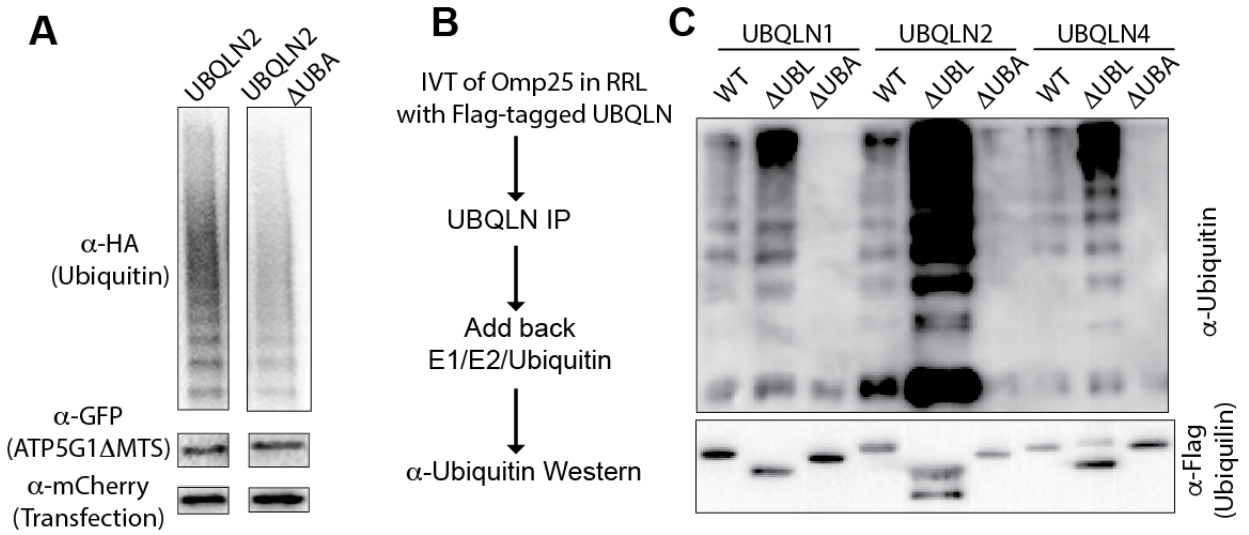

Figure 3: Substrate stabilization correlates with E3 ligase recruitment

a) TKO$^{UBQLN2\Delta UBA}$ cells have a decrease in ubiquitinated substrates. The GFP-ATP5G1ΔMTS-P2A-mCherry substrate was co-transfected with HA-Ubiquitin followed by an anti-GFP IP. Images cropped from the same western with the same contrast adjustment. UBQLN2 lane is the same one presented in Figure 2C.
b) Workflow for the *in vitro* ubiquitination assay.
c) *In vitro* ubiquitination assay shows that UBQLN2 has the most robust E3 ligase recruitment. ΔUBL was used as a positive control and ΔUBA was used as a negative control. Blot is overexposed to demonstrate that full-length Ubiquilin can recruit E3 ligases. See supplemental figure S2 for additional replicates of the assay.

<u>Ubiquilins recruit activated SCF^{bxo7}</u>

We next asked which E3 ligase(s) are recruited by Ubiquilins. We added recombinantly purified, flag-tagged full-length or ΔUBL UBQLN1 to RRL and performed an anti-flag IP. We then submitted the elution for mass spectrometry analysis. Our data set included Ube3A/E6AP, which was recently shown to interact with the Ubiquilin UBA domain[33]. We performed an immunoprecipitation with physiological levels of flag-tagged Ubiquilin in RRL, but were unable to observe an interaction with Ube3A. Considering that the K_D of this interaction is ~460 μM [33] and the assay used ~10 μM Ubiquilin, any interaction is likely below the detection limit of the assay.

We also observed Cul1 and the F-box protein Fbxo7 in our mass spec results, suggesting that Ubiquilins may also recruit SCF^{bxo7}. We again performed an IP with physiological levels of flag-tagged Ubiquilin added to RRL. We were able to validate Ubiquilin dependent recruitment of SCF components Cul1, Fbxo7 and Rbx1. Consistent with the results of the ubiquitination assay, UBQLN2 had the most robust recruitment of SCF^{bxo7} components **(Figure 4A)**.

To provide a functional validation of the interaction of Ubiquilins with SCF^{bxo7}, we repeated our ubiquitination assay in RRL treated with the Nedd8 specific protease NEDP1. SCF^{bxo7} activity requires neddylation of Cul1[47]. We hypothesized that if SCF^{bxo7} is the major E3 ligase recruited by Ubiquilins, then removal of Nedd8 from Cul1 should dramatically reduce ubiquitination activity. To test this hypothesis, we added the Nedd8 specific protease NEDP1 to the RRL prior to performing the anti-Flag IP with either full-length or ΔUBL UBQLN1. As expected, addition of NEDP1 collapsed almost the entire Cul1 signal down to a lower molecular weight band,

consistent with de-Neddylation activity **(Figure 4B)**. Interestingly, treatment with NEDP1 also leads to a substantial decrease in the amount of Cul1 bound to Ubiquilin, suggesting that Ubiquilins preferentially recruit the activated form of the enzyme. We then performed our ubiquitination assay with NEDP1 treated RRL. Treatment with NEDP1 led to a 40% reduction in ubiquitination activity **(Figure 4C & D)**. We conclude that SCF^{bxo7} is a major, but not the exclusive, E3 ligase recruited by Ubiquilins and that Ubiquilins can specifically recruit the activated form of this enzyme.

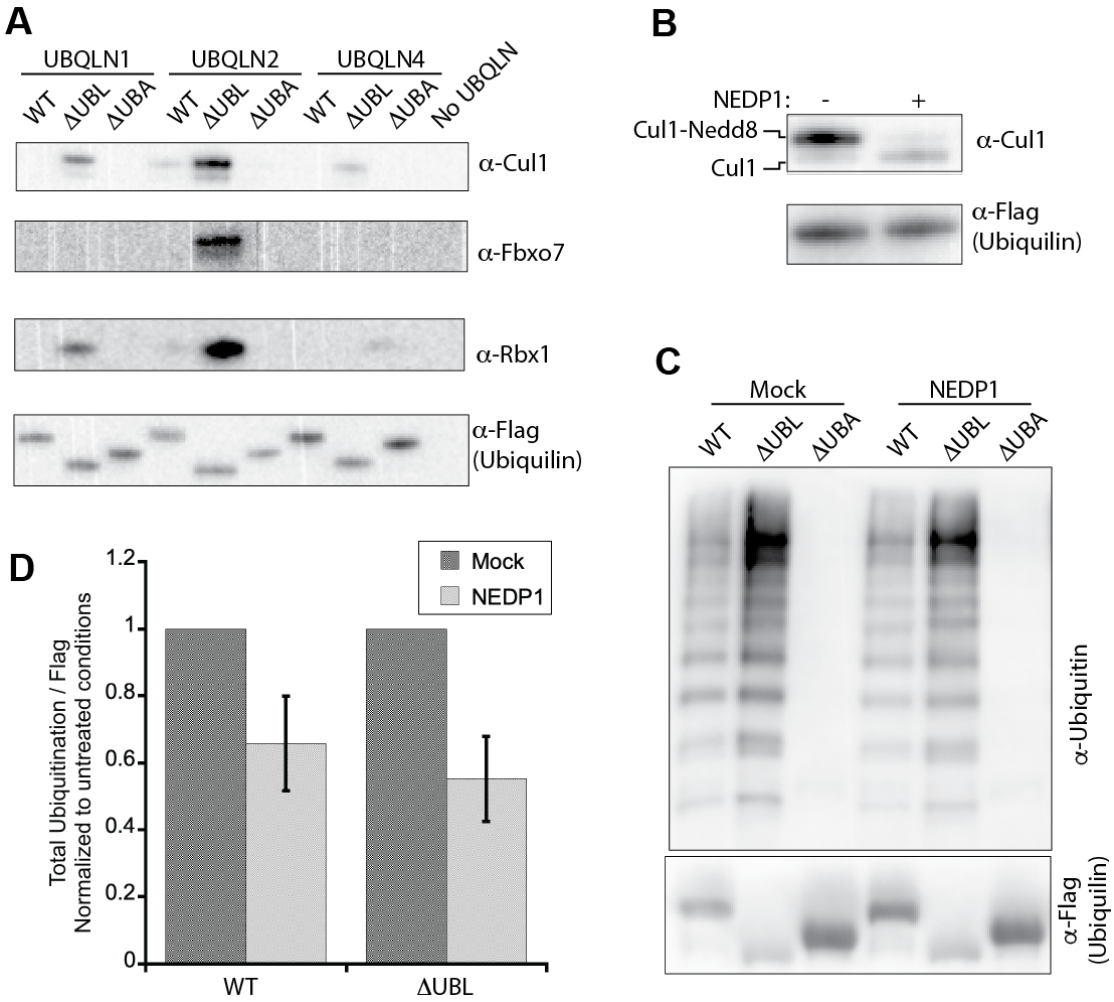

Figure 4: Ubiquilins recruit the E3 Ligase SCF^{bxo7}

a) Western blot validating interaction of Ubiquilins with components of the E3 ligase SCF^{bxo7}. Note that UBQLN2 has the most robust E3 ligase recruitment.
b) NEDP1 treatment leads to deneddylation of Cul1 and an overall decrease in the amount of Cul1 recruited by UBQLN2.
c) Treatment of RRL with NEDP1 leads to a drop in ubiquitination activity. Assay performed as in Figure 3B, except RRL was treated with NEDP1 before anti-Flag IP.
d) Quantification of blots in C (n = 3). Y axis is intensity of anti-ubiquitin blot divided by intensity of anti-flag blot.

UBQLN2 ALS mutants have defects in substrate stabilization that is exacerbated upon overexpression

To better understand how ALS mutants affect UBQLN2 activity, we developed TKO rescue cell lines for the following UBQLN2 ALS mutations: T487I, A488T, P497L, P506T, and P506A. We performed doxycycline titrations to obtain roughly physiological expression levels **(Figure S3)** and then measured substrate degradation using the GFP-ATP5G1ΔMTS-P2A-mCherry construct. All Ubiquilin variants were able to stabilize the substrate compared to WT and TKO cells. However, none of the ALS mutants were able to stabilize substrates to the same degree as TKO^{UBQLN2} **(Figure 5A)**. We then asked if overexpression of the ALS mutants could further stabilize the substrates. Surprisingly, we observed that overexpression of most mutants led to a decrease in substrate stabilization **(Figure S3D)**.

We next asked if the ALS mutants show a difference in their ability to recruit E3 ligases. We added recombinantly purified UBQLN2 ALS mutants to RRL and performed the *in vitro* ubiquitination assay. Total ubiquitination activity was comparable across all UBQLN2 disease mutants **(Figures 5B & C)**. Similarly, we observed only modest differences in Cul1 recruitment **(Figure S3E)**. We conclude that UBQLN2 ALS mutants have defects in substrate stabilization that are exacerbated upon UBQLN2 overexpression and that these defects in substrate stabilization are not due to differences in E3 ligase recruitment.

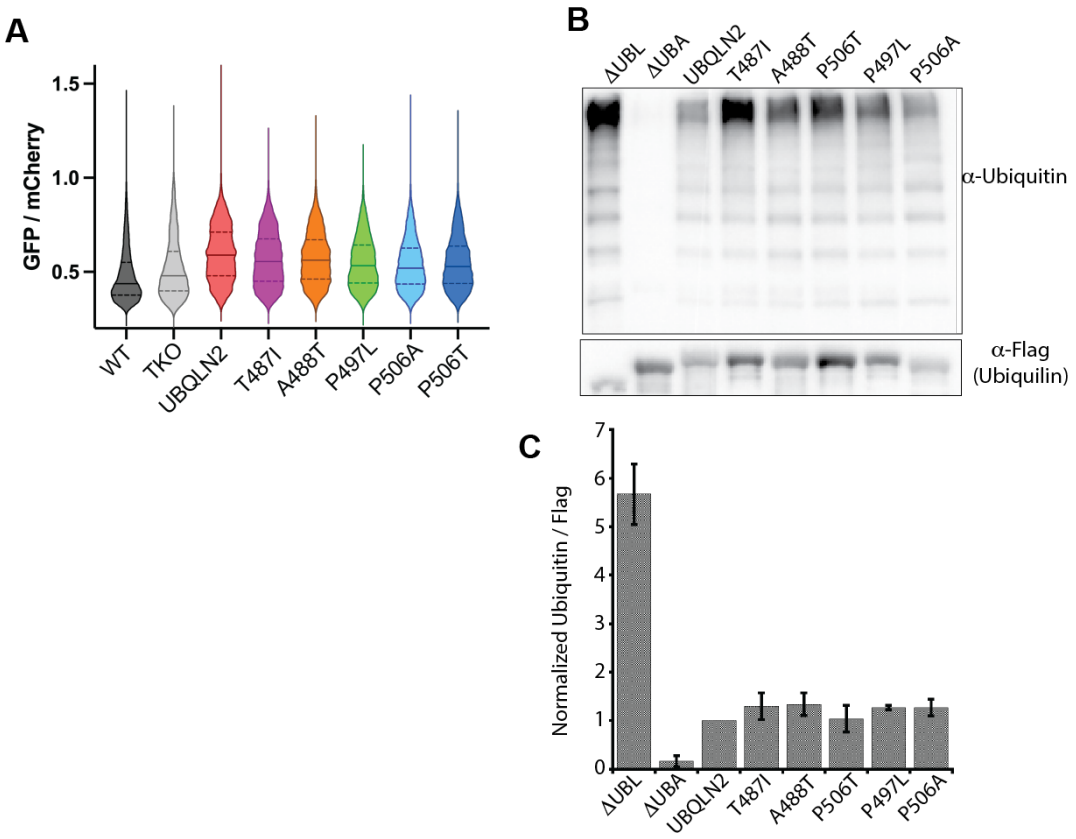

Figure 5: UBQLN2 ALS mutants have defects in substrate stabilization

A) All UBQLN2 ALS mutants can stabilize substrate, but show some defect compared with WT UBQLN2. TKO rescue cell lines were transformed with GFP-ATP5G1ΔMTS-P2A-mCherry.

B) In vitro ubiquitination assay shows no major differences in E3 ligase recruitment by UBQLN2 ALS mutants.
C) Quantification of B (n = 3). Y axis is intensity of anti-ubiquitin blot divided by intensity of anti-flag blot. Data is normalized such that wild type UBQLN2 has a value of 1.

Discussion

Despite clear links to neurodegenerative disease and decades of research, many fundamental aspects of Ubiquilin function remains unclear. What is the unique role of each Ubiquilin paralog? How can Ubiquilins selectively stabilize some substrates while promoting the degradation of others? What are the specific mechanistic defects in ALS mutants? What is the role of phase separation in Ubiquilin activity? Here, we have addressed these questions using a library of TKO rescue cell lines expressing a single Ubiquilin paralog or disease mutant under control of an inducible promoter. This system allowed us to mechanistically dissect the unique role of each paralog and disease mutant in a cellular setting while also avoiding experimental complications that accompany non-physiological Ubiquilin phase separation from transient overexpression.

Using this system, we demonstrate that UBQLN2 has a unique ability to protect substrates from proteasomal degradation, with the degree of stabilization correlating with UBQLN2 expression levels. The accumulation of ubiquitinated substrates in TKO^{UBQLN2} cells also correlates with the ability of UBQLN2 to recruit E3 ligases more robustly than other Ubiquilin paralogs. We identified SCF^{bxo7} as one of the major E3 ligases recruited by Ubiquilins. Interestingly, Ubiquilins appear to selectively recruit the activated form of SCF^{bxo7}, as removal of Nedd8, which is required for enzyme activation, leads to a significant drop in Ubiquilin binding. As NEDD8 is a ubiquitin like protein and E3 ligase recruitment depends on the UBA domain, Ubiquilins may recruit activated SCF^{bxo7} via a UBA-NEDD8 interaction, although more detailed studies are needed to validate this model.

Our data shows that UBQLN2 is distinct among the Ubiquilin paralogs in that it has an enhanced ability to act as a molecular chaperone that protects client proteins from degradation. It is tempting to speculate that the robust E3 ligase recruitment by UBQLN2 protects client proteins from degradation by promoting phase separation of Ubiquilin-substrate complexes **(Figure 6)**. While such a model still needs definitive experimental proof, it is appealing as it unifies several previous observations, including that: 1) Ubiquilins can protect some substrates from degradation[34–38], 2) polyubiquitin chains promote UBQLN2 phase separation[44–46], and 3) proteasome activity can be inhibited in UBQLN2 condensates[40,41].

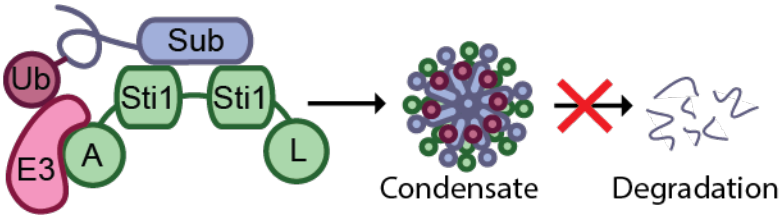

Figure 6: Proposed model of substrate stabilization by UBQLN2. UBQLN2 recruits E3 ligases via the UBA domain. Subsequent ubiquitination activity promotes formation of biomolecular condensates, which protects substrates from degradation.

One prediction of this model is that disruption of UBQLN2 phase separation should also disrupt UBQLN2 chaperone activity. As many UBQLN2 ALS mutants have altered phase separation properties[23,26], we decided to test the ability of these mutants to stabilize the model substrate ATP5G1ΔMTS. Interestingly, our results show that UBQLN2 ALS mutants have defects in

substrate stabilization that are exacerbated upon overexpression. Surprisingly, there is no change in overall E3 ligase recruitment. As Ubiquilin overexpression promotes phase separation, this model could account for the counterintuitive decrease in substrate stabilization upon overexpression of UBQLN2 ALS mutants. More work is needed to fully understand the role of phase separation in UBQLN2 function and how ALS mutations affect UBQLN2 function.

In summary, this study elucidates the distinct role of UBQLN2 among Ubiquilin paralogs in protecting substrates from proteasomal degradation. Counterintuitively, substrate stabilization correlates with the robust recruitment of E3 ligases such as SCF^{bxo7}. We propose that E3 ligase activity protects substrates from degradation by promoting the formation of biomolecular condensates. While this model requires definitive experimental validation, it synthesizes several observations from the literature and provides an exciting new paradigm for understanding UBQLN2 function in health and disease.

Materials and Methods

Cloning

The genes encoding Ubiquilins and associated variants were cloned into a pET28a vector with an N-terminal 6xHis tag followed by a 3C cleavage site and 3xFlag tag. Cloning was completed via Gibson Assembly for all Ubiquilin paralogs, disease mutants, and UBL/UBA truncations. Successful cloning was verified by Sanger sequencing.

For generation of stable cell lines, Ubiquilin variants were cloned into pcDNA5 mammalian expression vector containing an N-terminal 3xMyc tag with flanking FLP-FRT sequences for genomic integration. Cloning was completed via Gibson Assembly and restriction cloning. Successful cloning was verified by Sanger sequencing.

GFP-P2A-mCherry Dual Reporter plasmids were obtained courtesy of Manu Hedge and Sichen Shao. The genes encoding GFP-P2A-mCherry and GFP-ATP5G1ΔMTS-P2A-mCherry were cloned via restriction cloning into a pTK derivative (Thermo Fisher PI16151), under the control of the HSV TK promoter. Successful cloning was verified by Sanger sequencing.

Protein Purification

Plasmids encoding Ubiquilin variants were transformed into *E. coli* BL21(DE3) pRIL cells and expressed in Terrific Broth at 37° C to an OD_{600} of 0.6-0.8. Cultures were induced with 0.25 mM IPTG for 4.5 hours at 16° C. Cells were harvested by centrifugation at 3900 rpm, resuspended in Ubiquilin Lysis Buffer (50 mM Hepes pH 7.5, 150 mM NaCl, 0.01 mM EDTA, 10% glycerol, 20 mM imidazole), and supplemented with 1 mM PMSF, 0.05 mg/mL lysozyme (Alfa Aesar), and 500 U of Universal Nuclease (Pierce). Cells were lysed by sonication and supernatant was isolated by centrifugation for 30 min at 12,000 rpm. Supernatant was purified by Ni-NTA affinity chromatography (Thermo Fisher) by gravity flow. Ni-NTA resin was washed with 15 column volumes of Ubiquilin Lysis Buffer and eluted with 2 column volumes of Ubiquilin Lysis Buffer supplemented with 250 mM imidazole. Protein was dialyzed overnight at 4C against Ubiquilin Lysis Buffer supplemented with 3C Protease at a 1:100 ratio of protease to protein. Protein was passed over Ni-NTA resin to remove any uncleaved protein or Nickel binding contaminants. The flow through was collected and further purified by size exclusion chromatography on the Superdex 200 Increase 10/300 GL (GE Healthcare). Peak proteins were pooled and verified by denaturing SDS PAGE, concentrated to 60-100 μM using a 50kD MWCO centrifugal concentrator, aliquoted, flash frozen in LN2, and stored at -80° C. Protein concentration was measured by A280 and confirmed by Bradford assay.

Cell culture

Maintenance

HEK23TRex cells (TKO and WT) were maintained in DMEM supplemented with 10% FBS, 100 units/mL penicillin, 100 μg/mL streptomycin, 15 μg/mL Blasticidin, and 100 μg/mL Zeocin. HEK23TRex Rescue cells were maintained in DMEM supplemented with 10% FBS, 100 units/mL penicillin, 100 μg/mL streptomycin, 15 μg/mL Blasticidin, and 150 μg/mL Hygromycin. Cells were passaged every 2-3 days once reaching a confluency of 75-90%. Cells were not used further than passage 25.

Cell Lysis and Normalization

Cells were washed with DPBS, Trypsinized and centrifuged at 100g for 5 min. Cell pellets were lysed by mixing with the lysis buffer (25 mM Tris-HCl, pH 7.4, 150 mM NaCl, 1mM EDTA, 1% NP-40 and 5% Glycerol) supplemented with 125 Units/mL of universal nuclease (Pierce) and 1x Halt™ Protease Inhibitor Cocktail (Thermo Scientific). Lysates were centrifuged at 14,000 rpm for 15 min at 4° C and the supernatant was normalized by A280 with cell lysate dilution buffer (25 mM Tris-HCl, pH 7.4, 150 mM NaCl, 0.5 mM EDTA).

Induction of Ubiquilin expression

One day (24 h) prior to doxycycline addition, cells were split into 10 cm dishes in DMEM media and 10% FBS lacking antibiotics. Ubiquilin expression was induced by addition of doxycycline according to the table below. After 24 h in media with doxycycline, cells were harvested.

Cell line	Physiological expression	Overexpression
TKO^{UBQLN1}	10 ng/mL	n/a
TKO^{UBQLN2}	0.8 ng/mL	10 ng/mL
TKO^{UBQLN4}	10 ng/mL	n/a
TKO^{T487I}	0.5 ng/mL	10 ng/mL
TKO^{A488T}	2 ng/mL	10 ng/mL
TKO^{P497L}	6 ng/mL	10 ng/mL
TKO^{P506A}	5 ng/mL	10 ng/mL
TKO^{P506T}	4 ng/mL	10 ng/mL

Transfection

Transient transfection was conducted in 10 cm culture dishes. 24 hours prior to transfection, HEK293TRex cells were split into 10 cm dishes with DMEM supplemented with 10% FBS but lacking antibiotics. 36 μg of DNA was transfected into cells using 18 μL Lipofectamine 2000 (Invitrogen) in Opti-MEM (Gibco). For co-transfections with HA-Ubiquitin, 7.5 μg of the substrate and 4.5 μg of HA-Ubiquitin were transfected with 30 μL Lipofectamine 2000 (Invitrogen) in Opti-MEM (Gibco). Opti-MEM media was exchanged for DMEM supplemented with 10% FBS but lacking antibiotics 4-5 hours following transfection. For experiments in which Ubiquilins were induced with Doxycycline, the media for the media change was supplemented with doxycycline according to the above table. Cells were harvested for subsequent analysis or experiment 24 hours following transfection.

Generation and validation of TKO rescue cell lines

TKO HEK293TRex cells were obtained courtesy of Manu Hegde and were generated as described previously[32]. TKO cells were transfected, as described above, in 6 well plates. 0.6 μg 3xMyc-Ubiquilin was co-transfected with 5.4 μg pOG44 at a 9:1 ratio of pOG44 to plasmid in Opti-MEM (Gibco) using 3 μL Lipofectamine 2000 (Invitrogen). Opti-MEM media was

exchanged for DMEM supplemented with 10% FBS but lacking antibiotics for 4-5 hours following transfection. 24 hours following transfection, media was exchanged for fresh DMEM with 10% FBS. 48 hours following transfection, cells were split into 10 cm culture dishes and cultured in DMEM supplemented with 10% FBS, 100 units/mL penicillin, 100 μg/mL streptomycin, 15 μg/mL Blasticidin, and 150 μg/mL Hygromycin (Gibco). Cells were frozen following 17-21 days of antibiotic selection. Expression of transfected species was verified by western blots (anti-Myc and anti-Ubiquilin) as well as PCR amplification and sequencing.

Immunoprecipitation

From RRL

30 μL of anti-Flag magnetic resin (Pierce) was washed in Flag Pulldown Buffer (25 mM HEPES, 250 mM KOAc, 0.1% Tween 20). RRL containing Flag-tagged Ubiquilin was incubated with resin at 4° C for 1 hour. Flow through was discarded, and resin was further washed in Flag Pulldown Buffer. Bound proteins were eluted with 1 mg/mL Flag Peptide (ApexBio) at 37° C on thermomixer.

From cells

Magnetic resin (anti-GFP, Proteintech) was washed in Cell Lysate IP Wash Buffer (25 mM Tris-HCl, 150 mM NaCl, 0.5 mM EDTA, 0.1% Tween 20). Cell Lysates were incubated with resin at 4° C for 1 hour. Flow through was discarded, and resin was further washed with Cell Lysate IP Wash Buffer. For anti-GFP resin, bound proteins were eluted with 1x SDS buffer at 95° C for 5 minutes on a thermomixer.

Cell Viability Assay

Cells were maintained in 6 well plates with the growth conditions as described and counted every 24 hours from seeding for 4 consecutive days. Cells were harvested and pelleted as described and the pellets were dissolved in DPBS. The cell suspension was mixed with 4% Trypan blue (Gibco) at a 1:1 ratio and the cells were counted using a hemocytometer.

Flow Cytometry Degradation Assays

HEK293TRex Cell Lines were transfected as described above in 10 cm dishes with GFP-P2A-mCherry dual reporter plasmids. TKO rescue cell lines were induced with indicated levels of doxycycline 4-5 hours following transfection. 24 hours following transfection, cells were washed in 10 mL DPBS, trypsinized, and centrifuged at 100 x g for 5 minutes. Cells were resuspended in DPBS and filtered via 40/50 um filter into 5 mL tubes. Cells were stained in 3 μM DAPI (Invitrogen). Flow Cytometry was completed on BioRad ZE5 Cell Analyzer or BD Biosciences LSR15 cytometer, and further analysis was completed using FlowJo.

Ubiquitination Assay

RRL IVT

RRL *in vitro* transcription and translation was performed as described previously[48]. DEPC water was used throughout the protocol. Omp25 IVT optimized plasmid was transcribed via T7 polymerase in the presence of RNase inhibitor (Invitrogen) for 1 hour at 37° C. Translation was carried out at 32° C for 30 minutes in the presence of recombinantly expressed, purified Ubiquilins at a concentration of 10.4 μM. Translation was supplemented with 5 μM methionine.

In vitro Ubiquitination

Ubiquitination of IVT reaction products was performed as described previously[32]. 4x Ubiquitination Mix was assembled using 40 μM His-ubiquitin (R&D Systems), 0.4 μM GST-Ube1 (R&D Systems), 1.2 μM UbcH5a (R&D Systems), and an energy regenerating system (4 mM

ATP (Thermo Scientific), 40 mM Creatine Phosphate (Thermo Scientific), and 160 μg/mL Creatine Kinase. Ubiquitination was performed for 1 hour at 37° C on thermomixer, followed by termination in 1% SDS at 95C for 10 minutes on thermomixer.

NEDP1

For experiments in which NEDP1 treatment was used, RRL was incubated with 10 μM His-NEDP1 (Southbay Bio) at 37° C for 30 minutes on thermomixer. Treated RRL was used in subsequent ubiquitination or immunoprecipitation experiments.

Western blots

SDS PAGE was performed using 4% stacking, 15% separating Tris-Glycine gels (cast in house) (Figure 2B), 4–20% Mini-PROTEAN TGX Precast Protein Gels (Bio-Rad), 4–20% Criterion TGX Stain-Free Protein Gels (Bio-Rad). Gels were transferred to 0.45 um PVDF transfer membrane (Thermo Scientific) at 4° C for 1 hour at 330 mA in 1x Transfer Buffer (192 mM Glycine, 25 mM Tris-Base, 0.01% SDS, in MeOH) or using the Trans-Blot Turbo Transfer System (BioRad) at mixed molecular weight settings for 10 minutes. Blocking was completed in 5% milk, antibody incubations in 1% milk, and washing in 1x TBST (20 mM Tris-Base, 200 mM NaCl, 0.1% Tween-20, pH 7.4), all using standard techniques. Antibody dilutions can be found in the Key Resources Table below. Blots were developed using Cytiva Amersham ECL Select Western Blotting Detection Reagent (Cytiva) or SuperSignal West Femto Maximum Sensitivity Substrate (Thermo Scientific).

Key Resources Table

Reagent or Resource	**Source**	**Identifier (Catalog # or RRID)**
Antibodies		
Mouse monoclonal anti-ubiquitin (1:1,500 dilution)	Invitrogen (via ThermoFisher)	Cat. #14-6078-82; RRID: AB_837154
Mouse monoclonal anti-Flag (1:5,000 dilution)	GenScript	Cat. #A00187; RRID: AB_1720813
Mouse monoclonal anti-FBXO7 (1:1,000 dilution)	Santa Cruz Biotechnology	Cat. #sc-271763; RRID: AB_10708586
Mouse monoclonal anti-Cullin1 (1:500 dilution)	Invitrogen (via ThermoFisher)	Cat. #32-2400; RRID: AB_2533070
Mouse monoclonal anti-RBX1 (1:20,000 dilution)	Proteintech	Cat. #66716-1-Ig; RRID: AB_2882067
Mouse monoclonal anti-actin (1:10,000 dilution)	Invitrogen (via ThermoFisher)	Cat. #MA1-744; RRID: AB_2223496
Mouse monoclonal anti-c-Myc (1:1,000 dilution)	Santa Cruz Biotechnology	Cat. #sc-40; RRID: AB_627268
Rabbit monoclonal anti-c-Myc (1:5,000 dilution)	Invitrogen (via ThermoFisher)	Cat. #700648; RRID: AB_2532334
Mouse monoclonal anti-GFP (1:3,000 dilution)	Invitrogen (via ThermoFisher)	Cat. #MA5-15256; RRID: AB_10979281
Rabbit polyclonal anti-mCherry (1:10,000 dilution)	Invitrogen (via ThermoFisher)	Cat. #PA5-34974; RRID: AB_2552323
Mouse monoclonal anti-UBQLN2 (Clone 5F5) (1:1,000 dilution)	Sigma-Aldrich	Cat. #WH0029978M3-100UG; RRID: AB_1841365

Rabbit polyclonal anti-CIP75 (UBQLN4) (1:1,000 dilution)	Abcam	Cat. #ab106443; RRID: AB_10866635
Goat polyclonal HRP anti-mouse (1:10,000 dilution)	Invitrogen (via ThermoFisher)	Cat. #31430; RRID: AB_228307
Goat polyclonal HRP anti-rabbit (1:10,000 dilution)	Proteintech	Cat. #SA00001-2; RRID: AB_2722564
Bacterial and Virus Strains		
E. coli DH5-5α competent cells	ThermoFisher	Cat. #EC0112
E. coli BL21 (DE3) pRIL competent cells	Agilent	Cat. #230245
Cell lines		
HEK293TRex TKO	Itakura et al. 2016[32]	
Chemicals, Peptides, Recombinant Proteins		
SuperSignal West Femto Maximum Sensitivity Substrate	Thermo Scientific	Cat. #34095
Cytiva Amersham ECL Select Western Blotting Detection Reagent	Cytiva (via Fisher Scientific)	Cat. #45-000-999
PVDF Transfer Membrane, 0.45 µm, 26.5 cm x 3.75 m	Thermo Scientific	Cat. #88518
4–20% Criterion TGX Stain-Free Protein Gel	Bio-Rad	Cat. #5678095
4–20% Mini-PROTEAN TGX Precast Protein Gels	Bio-Rad	Cat. #4561096
3–8% Criterion XT Tris-Acetate Protein Gel	Bio-Rad	Cat. #3450131
T7 Polymerase	Purified in lab	N/A
SUPERase-In RNase Inhibitor	Invitrogen (via Thermo Fisher)	CAT. #AM2696
His6-Ubiquitin	R&D Systems	Cat. #U-530
GST-Ube1 (E1)	R&D Systems	Cat. #E-306-050
UbcH5a (E2)	R&D Systems	Cat. #E2-616-100
ATP		
Creatine phosphate disodium salt tetrahydrate, 99%	Thermo Scientific	Cat. #AC337340010
Anti-DYKDDDDK Magnetic Agarose	Pierce (via ThermoFisher)	Cat. #PIA36797
3X (DYKDDDDK) Peptide	APExBIO	Cat. #A6001
Anti-C-Myc Magnetic Beads	Sigma-Aldrich	Cat. #SAE0201
c-Myc Peptide	GenScript	Cat. #RP11731
ChromoTek GFP-Trap® Magnetic Agarose	Proteintech	Cat. #gtma
Doxycycline Hydrochloride	Fisher Scientific	Cat. #BP26535
Zeocin Selection Reagent	Invitrogen (via ThermoFisher)	Cat. #R25001

Hygromycin B	Invitrogen (via ThermoFisher)	Cat. #10687010
Blasticidin	Gibco (via ThermoFisher)	Cat. #A1113902
Pen/Strep	Gibco (via ThermoFisher)	Cat. #15140122
DMEM	Gibco (via ThermoFisher)	Cat. #10569044
Optimem	Gibco (via ThermoFisher)	Cat. #51985034
DPBS	Gibco (via ThermoFisher)	Cat. #14190235
DAPI (4',6-Diamidino-2-Phenylindole, Dilactate)	Invitrogen (via ThermoFisher)	Cat. #10687010
Trypan Blue	Gibso (via ThermoFisher)	Cat. #15250061
Recombinant DNA		
His-3C-3xFLAG-UBQLN1 (pET28a)	This study	N/A
His-3C-3xFLAG-UBQLN1 (ΔUBL) (pET28a)	This study	N/A
His-3C-3xFLAG-UBQLN1 (ΔUBA) (pET28a)	This study	N/A
His-3C-3xFLAG-UBQLN2 (pET28a)	This study	N/A
His-3C-3xFLAG-UBQLN2 (ΔUBL) (pET28a)	This study	N/A
His-3C-3xFLAG-UBQLN1 (ΔUBA) (pET28a)	This study	N/A
His-3C-3xFLAG-UBQLN4 (pET28a)	This study	N/A
His-3C-3xFLAG-UBQLN4 (ΔUBL) (pET28a)	This study	N/A
His-3C-3xFLAG-UBQLN4 (ΔUBA) (pET28a)	This study	N/A
His-3C-3xFLAG-UBQLN2 A488T (pET28a)	This study	N/A
His-3C-3xFLAG-UBQLN2 T487I (pET28a)	This study	N/A
His-3C-3xFLAG-UBQLN2 P497L (pET28a)	This study	N/A
His-3C-3xFLAG-UBQLN2 p506A (pET28a)	This study	N/A
His-3C-3xFLAG-UBQLN2 P506T (pET28a)	This study	N/A
pTK-GFP-NheI-P2A-mCherry (HSV pTK)	Itakura et al. 2016[32]	N/A
pTK-GFP-ATP5G1 (ΔMTS)-P2A-mCherry (HSV pTK)	This study	N/A
3xMyc-UBQLN1 (pcDNA5)	Itakura et al. 2016[32]	
3xMyc-UBQLN2 (pcDNA5)	This study	N/A
3xMyc-UBQLN2 ΔUBA (pcDNA5)	This study	N/A
3xMyc-UBQLN2 (pcDNA5)	This study	N/A
3xMyc-UBQLN4 (pcDNA5)	This study	N/A

3xMyc-UBQLN2 T487I (pcDNA5)	This study	N/A
3xMyc-UBQLN2 A488T (pcDNA5)	This study	N/A
3xMyc-UBQLN2 P497L (pcDNA5)	This study	N/A
3xMyc-UBQLN2 P506A (pcDNA5)	This study	N/A
3xMyc-UBQLN2 P506T (pcDNA5)	This study	N/A

Acknowledgements
The authors wish to thank the Hegde, Shao, and Castañeda labs for the TKO knockout cell line, plasmids, and helpful discussions. The authors also acknowledge Shawn Allen for help in maintaining the cell lines and the flow cytometry cores at the University of Michigan and University of Pittsburgh.
Funding: This work was supported by NSF CAREER Award 2343131 (MLW).
Author Contributions: Conceptualization: AS, ST, GS, MLW; Methodology: AS, ST, GS; Investigation: AS, ST, GS; Writing – Original Draft: AS, MLW; Writing – Review and Editing: AS, ST, GS, MLW; Supervision and Funding Acquisition: MLW
Competing Interests: The authors declare no competing interests.

Supplemental Figures

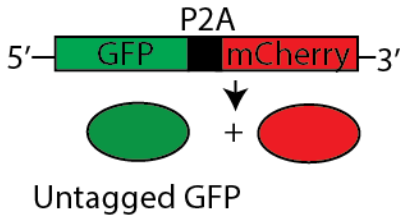

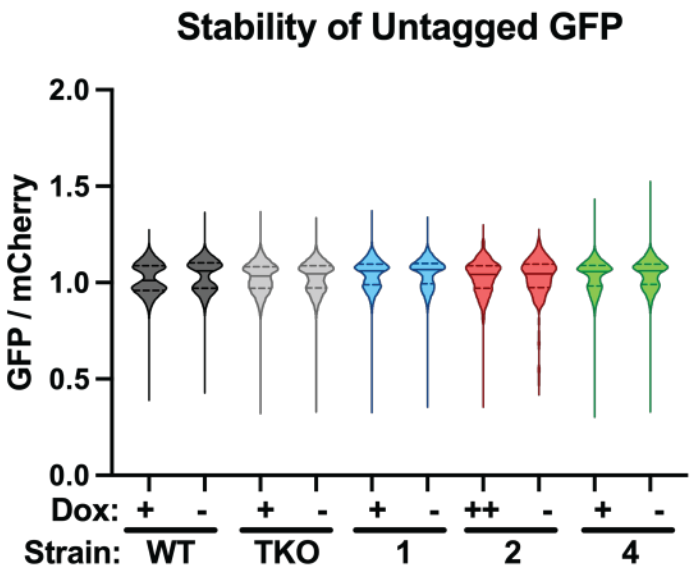

Figure S1: Untagged control for GFP:mCherry assay

A) Diagram of assay
B) Untagged GFP and mCherry are equally stable in all cell lines. Doxycycline concentrations were sufficient to give physiological Ubiquilin expression (+) or overexpression (++).

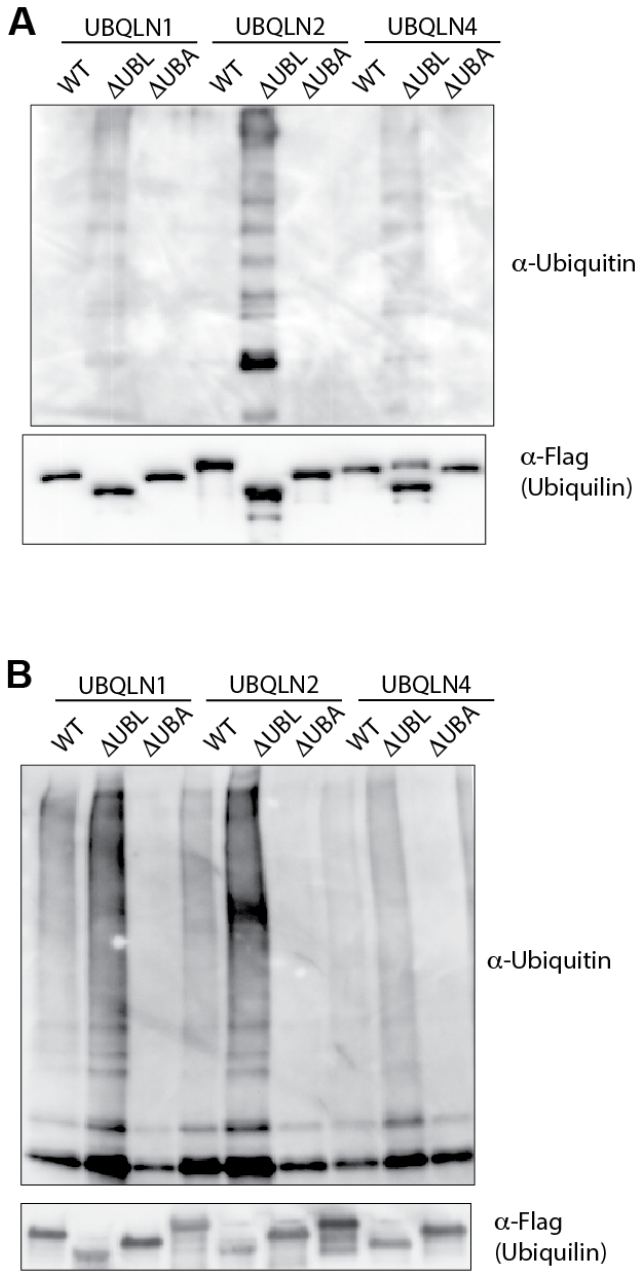

Figure S2: Additional replicates of the *in vitro* ubiquitination assay.
In vitro ubiquitination assay was performed as in figure 3. These are three different replicates performed with different stocks of purified Ubiquilins.

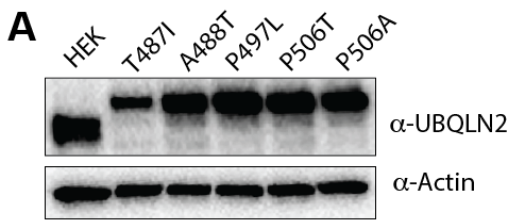

B

Mutant	[Dox]
T487I	0.5
A488T	2
P497L	6
P506A	5
P506T	4

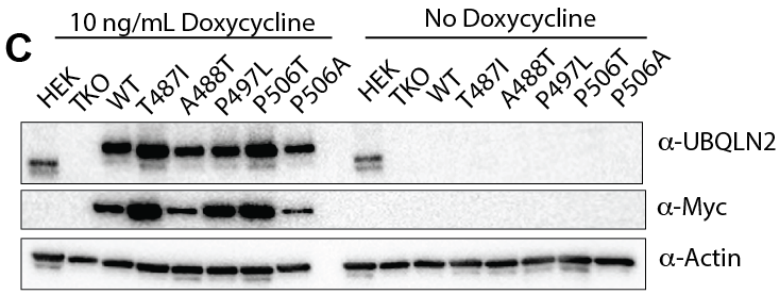

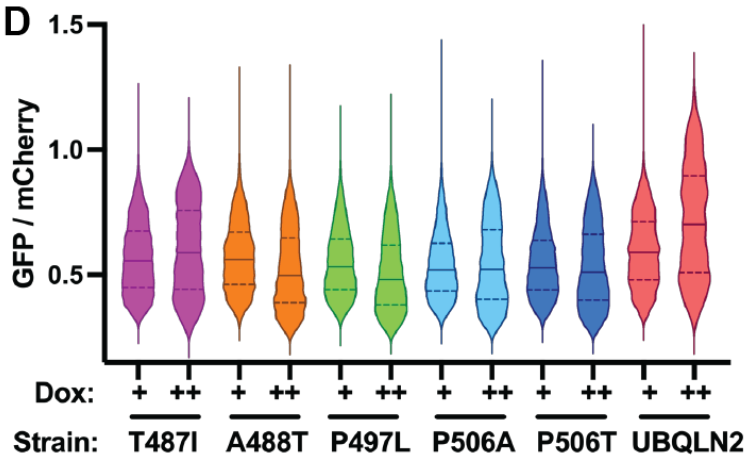

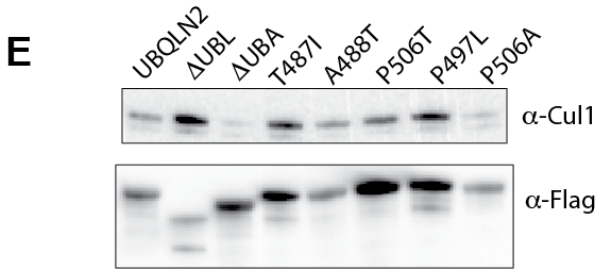

Figure S3: Characterization of UBQLN2 ALS Mutants

A) Anti-UBQLN2 western blot showing roughly physiological expression of ALS mutants
B) Table showing the concentration of doxycycline (ng/mL) used in A.
C) Anti-UBQLN2 and anti-Myc western blots of ALS mutants under overexpression conditions (10 ng/mL doxycycline)

D) Overexpression of UBQLN2 ALS mutants leads to decreased substrate stability. Assay performed as in Figure 5A, but with physiological Ubiquilin expression (+) or overexpression (++).
E) UBQLN2 ALS mutants show no major differences in binding to Cul1 when normalized to UBQLN2 concentration. Flag-tagged UBQLN2 ALS mutants were immunoprecipitated from RRL.

References

1. Hegde, R. S. & Zavodszky, E. Recognition and Degradation of Mislocalized Proteins in Health and Disease. *Csh Perspect Biol* **11**, a033902 (2019).

2. Phillips, B. P. & Miller, E. A. Membrane protein folding and quality control. *Curr Opin Struc Biol* **69**, 50–54 (2021).

3. Song, J., Herrmann, J. M. & Becker, T. Quality control of the mitochondrial proteome. *Nat Rev Mol Cell Bio* **22**, 54–70 (2021).

4. Jiang, H. Quality control pathways of tail-anchored proteins. *Biochimica Et Biophysica Acta Bba - Mol Cell Res* **1868**, 118922 (2020).

5. Fresenius, H. L. & Wohlever, M. L. Sorting out how Msp1 maintains mitochondrial membrane proteostasis. *Mitochondrion* **49**, 128–134 (2019).

6. Anoar, S., Woodling, N. S. & Niccoli, T. Mitochondria Dysfunction in Frontotemporal Dementia/Amyotrophic Lateral Sclerosis: Lessons From Drosophila Models. *Front. Neurosci.* **15**, 786076 (2021).

7. Martin, L. J. Biology of mitochondria in neurodegenerative diseases. *Progress in molecular biology and translational science* **107**, 355–415 (2012).

8. Labbadia, J. & Morimoto, R. I. The biology of proteostasis in aging and disease. *Annual review of biochemistry* **84**, 435–464 (2015).

9. Harbauer, A. B., Zahedi, R. P., Sickmann, A., Pfanner, N. & Meisinger, C. The protein import machinery of mitochondria-a regulatory hub in metabolism, stress, and disease. *Cell metabolism* **19**, 357–372 (2014).

10. Wang, W., Zhao, F., Ma, X., Perry, G. & Zhu, X. Mitochondria dysfunction in the pathogenesis of Alzheimer's disease: recent advances. *Mol. Neurodegener.* **15**, 30 (2020).

11. Douglas, P. M. & Dillin, A. Protein homeostasis and aging in neurodegeneration. *J. Cell Biol.* **190**, 719–729 (2010).

12. Winter, J. M. *et al.* Collateral deletion of the mitochondrial AAA+ ATPase ATAD1 sensitizes cancer cells to proteasome dysfunction. *Elife* **11**, e82860 (2022).

13. Zheng, T., Yang, Y. & Castañeda, C. A. Structure, dynamics and functions of UBQLNs: at the crossroads of protein quality control machinery. *Biochem J* **477**, 3471–3497 (2020).

14. Black, H. H. *et al.* UBQLN2 restrains the domesticated retrotransposon PEG10 to maintain neuronal health in ALS. *Elife* **12**, e79452 (2023).

15. Ma, Q. *et al.* UBQLN2 and HSP70 participate in Parkin-mediated mitophagy by facilitating outer mitochondrial membrane rupture. *EMBO Rep.* e55859 (2023) doi:10.15252/embr.202255859.

16. Gerson, J. E. *et al.* Ubiquilin-2 differentially regulates polyglutamine disease proteins. *Hum Mol Genet* **29**, 2596–2610 (2020).

17. Hjerpe, R. *et al.* UBQLN2 Mediates Autophagy-Independent Protein Aggregate Clearance by the Proteasome. *Cell* **166**, 935–949 (2016).

18. Şentürk, M. *et al.* Ubiquilins regulate autophagic flux through mTOR signalling and lysosomal acidification. *Nature cell biology* **21**, 384–396 (2019).

19. Lin, B. C., Higgins, N. R., Phung, T. H. & Monteiro, M. J. UBQLN proteins in health and disease with a focus on UBQLN2 in ALS/FTD. *Febs J* (2021) doi:10.1111/febs.16129.

20. Sharkey, L. M. *et al.* Modeling UBQLN2-mediated neurodegenerative disease in mice: Shared and divergent properties of wild type and mutant UBQLN2 in phase separation, subcellular localization, altered proteostasis pathways, and selective cytotoxicity. *Neurobiol Dis* **143**, 105016 (2020).

21. Alexander, E. J. *et al.* Ubiquilin 2 modulates ALS/FTD-linked FUS–RNA complex dynamics and stress granule formation. *Proceedings of the National Academy of Sciences* **5**, 201811997 (2018).

22. Deng, H.-X. *et al.* Mutations in UBQLN2 cause dominant X-linked juvenile and adult-onset ALS and ALS/dementia. *Nature* **477**, 211–215 (2011).

23. Riley, J. F., Fioramonti, P. J., Rusnock, A. K., Hehnly, H. & Castañeda, C. A. ALS-linked mutations impair UBQLN2 stress-induced biomolecular condensate assembly in cells. *J Neurochem* (2021) doi:10.1111/jnc.15453.

24. Lin, B. C. *et al.* ALS/FTD mutations in UBQLN2 are linked to mitochondrial dysfunction through loss-of-function in mitochondrial protein import. *Hum Mol Genet* (2021) doi:10.1093/hmg/ddab116.

25. Fahed, A. C. *et al.* UBQLN2 Mutation Causing Heterogeneous X-linked Dominant Neurodegeneration. *Annals of neurology* (2014) doi:10.1002/ana.24164.

26. Safren, N. *et al.* Pathogenic mutations in UBQLN2 exhibit diverse aggregation propensity and neurotoxicity. *Sci. Rep.* **14**, 6049 (2024).

27. Sandoval-Pistorius, S. S. *et al.* Ubiquilin-2 regulates pathological alpha-synuclein. *Sci Rep-uk* **13**, 293 (2023).

28. Idera, A. *et al.* Wild-type and pathogenic forms of ubiquilin 2 differentially modulate components of the autophagy-lysosome pathways. *J. Pharmacol. Sci.* **152**, 182–192 (2023).

29. Gerson, J. E. *et al.* Disrupting the Balance of Protein Quality Control Protein UBQLN2 Accelerates Tau Proteinopathy. *J Neurosci* **42**, 1845–1863 (2022).

30. Kleijnen, M. F. *et al.* The hPLIC proteins may provide a link between the ubiquitination machinery and the proteasome. *Molecular Cell* **6**, 409–419 (2000).

31. Walters, K. J., Kleijnen, M. F., Goh, A. M., Wagner, G. & Howley, P. M. Structural studies of the interaction between ubiquitin family proteins and proteasome subunit S5a. *Biochemistry* **41**, 1767–1777 (2002).

32. Itakura, E. *et al.* Ubiquilins Chaperone and Triage Mitochondrial Membrane Proteins for Degradation. *Molecular Cell* **63**, (2016).

33. Buel, G. R. *et al.* E6AP AZUL interaction with UBQLN1/2 in cells, condensates, and an AlphaFold-NMR integrated structure. *Structure* **31**, 395-410.e6 (2023).

34. Kurlawala, Z. *et al.* Ubiquilin proteins regulate EGFR levels and activity in lung adenocarcinoma cells. *J Cell Biochem* **122**, 43–52 (2021).

35. Ayadi, A. E., Stieren, E. S., Barral, J. M. & Boehning, D. Ubiquilin-1 regulates amyloid precursor protein maturation and degradation by stimulating K63-linked polyubiquitination of lysine 688. *Proceedings of the National Academy of Sciences* **109**, 13416–13421 (2012).

36. Stieren, E. S. *et al.* Ubiquilin-1 Is a Molecular Chaperone for the Amyloid Precursor Protein. *Journal of Biological Chemistry* **286**, 35689–35698 (2011).

37. Mah, A. L., Perry, G., Smith, M. A. & Monteiro, M. J. Identification of ubiquilin, a novel presenilin interactor that increases presenilin protein accumulation. *The Journal of Cell Biology* **151**, 847–862 (2000).

38. Adegoke, O. O. *et al.* Overexpression of Ubiquilin-1 Alleviates Alzheimer's Disease-Caused Cognitive and Motor Deficits and Reduces Amyloid-β Accumulation in Mice. *J. Alzheimer's Dis.* **Preprint**, 1–16 (2017).

39. Mohan, H. M. *et al.* RTL8 promotes nuclear localization of UBQLN2 to subnuclear compartments associated with protein quality control. *Cell Mol Life Sci* **79**, 176 (2022).

40. Valentino, I. M. *et al.* Phase separation of polyubiquitinated proteins in UBQLN2 condensates controls substrate fate. *bioRxiv* 2024.03.15.585243 (2024) doi:10.1101/2024.03.15.585243.

41. Waite, K. A., Vontz, G., Lee, S. Y. & Roelofs, J. Proteasome condensate formation is driven by multivalent interactions with shuttle factors and ubiquitin chains. *Proc. Natl. Acad. Sci.* **121**, (2024).

42. Dao, T. P. *et al.* ALS-Linked Mutations Affect UBQLN2 Oligomerization and Phase Separation in a Position- and Amino Acid-Dependent Manner. *Structure* **27**, 937-951.e5 (2019).

43. Felipe, P. de *et al.* E unum pluribus: multiple proteins from a self-processing polyprotein. *Trends Biotechnol.* **24**, 68–75 (2006).

44. Dao, T. P. *et al.* Mechanistic insights into enhancement or inhibition of phase separation by different polyubiquitin chains. *Embo Rep* **23**, e55056 (2022).

45. Dao, T. P. & Castañeda, C. A. Ubiquitin-Modulated Phase Separation of Shuttle Proteins: Does Condensate Formation Promote Protein Degradation? *Bioessays* **42**, 2000036 (2020).

46. Dao, T. P. *et al.* Ubiquitin Modulates Liquid-Liquid Phase Separation of UBQLN2 via Disruption of Multivalent Interactions. *Molecular Cell* **69**, 965-978.e6 (2018).

47. Deshaies, R. J. & Joazeiro, C. A. P. RING Domain E3 Ubiquitin Ligases. *Annu Rev Biochem* **78**, 399–434 (2009).

48. Sharma, S. K., Rios, P. D. los, Christen, P., Lustig, A. & Goloubinoff, P. The kinetic parameters and energy cost of the Hsp70 chaperone as a polypeptide unfoldase. *Nature chemical biology* **6**, 914–920 (2010).